AGU PUBLICATIONS

Geophysical Research Letters

RESEARCH LETTER

10.1002/2015GL064593

Key Points:

- The 1 year 2014 California drought was a multicentury-scale event
- The cumulative 2012–2014 California drought was a multimillennial-scale event
- The relative severity of the cumulative 2012–2015 drought is unprecedented

Supporting Information:

- Figures S1–S8

Correspondence to:
S. M. Robeson,
srobeson@indiana.edu

Citation:
Robeson, S. M. (2015), Revisiting the recent California drought as an extreme value, *Geophys. Res. Lett.*, *42*, doi:10.1002/2015GL064593.

Received 16 MAY 2015
Accepted 28 JUL 2015
Accepted article online 31 JUL 2015

Revisiting the recent California drought as an extreme value

Scott M. Robeson[1]

[1]Department of Geography and Department of Statistics, Indiana University, Bloomington, Bloomington, Indiana, USA

Abstract Spatially weighted averages of Palmer Drought Severity Index (PDSI) over central and southern California show that the 1 year 2014 drought was not as severe as previously reported, but it still is the most severe in the 1895–2014 instrumental record. Using the typical adjustment procedure that matches the mean and standard deviation of tree ring PDSI values to those of instrumental data shows over 10 droughts from 800 to 2006 that were more severe than the 1 year 2014 drought, with the 2014 drought having a return period of 140–180 years. Quantile mapping allows for a closer correspondence between instrumental and tree ring PDSI probability distributions and produces return periods of 700–900 years for the 1 year 2014 drought. Associated cumulative 3 and 4 year droughts, however, are estimated to be much more severe. The 2012–2014 drought is nearly a 10,000 year event, while the 2012–2015 drought has an almost incalculable return period and is completely without precedent.

1. Introduction

Interannual variations and persistence of drought conditions are profoundly important for human activities and natural ecosystems. Recent drought conditions in California have been particularly intense and have been analyzed using instrumental data, paleoclimatic proxies, and modeling approaches [*Diffenbaugh et al.*, 2015; *Griffin and Anchukaitis*, 2014; *Funk et al.*, 2014; *Swain et al.*, 2014]. A recent article in GRL by *Griffin and Anchukaitis* [2014] (hereafter GA14) produced the important finding that the Palmer Drought Severity Index (PDSI) for central and southern California during 2014 was likely the most severe in 1200+ years (residual-based error analysis also showed a number of other drought years that were similar in magnitude to 2014). The purpose of this article is to evaluate the impacts of a spatial averaging error in their calculation of California's instrumental PDSI value and to expand on the recent drought from the perspective of extreme value theory. As a result, the approach used here is based on that of GA14, except that spatial averages of central and southern California's drought conditions are weighted by the area represented by the instrumental data. In addition, the empirical probability distribution of the long-term tree ring record is readjusted and reevaluated using quantile mapping, which provides a closer match of the tree ring record to the instrumental data. Extreme value analysis is then used to estimate return periods and the expected frequency of conditions as severe as (1) the 2014 drought, (2) the cumulative 2012–2014 drought, and (3) an estimate of the cumulative 2012–2015 drought.

2. Data and Methods

Based on GA14, the analyses presented here use averages of the June/July/August (JJA) Palmer Drought Severity Index (PDSI) obtained from (1) NOAA's 1895 to 2015 climate division (instrumental) data for California [*Vose et al.*, 2014] and (2) version 2a of the North American Drought Atlas (NADA), which is a gridded reconstruction of PDSI based on tree ring records that extend back more than 1200 years [*Cook et al.*, 2004, 2008]. The JJA period matches the instrumental data to the long-term tree ring record and the highly persistent nature of PDSI allows for a close representation of several months prior to JJA for a given year [*Guttman*, 1998; *Heim*, 2005], including the bulk of each water year's wet season. As in GA14, climate divisions 4 to 7, which cover most of central and southern California, are used (Figure S1 in the supporting information). For the NADA data, GA14 reported the use of data from just three gridded values (red plusses in Figure S1). Here spatial averages of the NADA data using all grid boxes that overlap with the NOAA climate divisions (Figure S1) are used to ensure coverage of the same region as the instrumental data.

One fundamental difference in the analysis here is the weighting of the instrumental data by the area of each NOAA climate division to form a spatial average over the region. Area-based weighting is a particularly important step in the western U.S., where NOAA climate divisions are vastly different in size. The four NOAA climate divisions used here (Figure S1) have the following areas: 27,415 km^2 (Division 4, Central Coast); 85,777 km^2 (Division 5, San Joaquin); 36,332 km^2 (Division 6, South Coast); and 118,206 km^2 (Division 7, Southeast Desert). The 2.5° × 2.5° latitude-longitude grid used with the NADA reconstruction also requires a weighted average to account for the differential size of grid points and their fractional overlap with the climate divisions. While areal weighting is widely used for estimating spatial means, it is essential for estimating any statistical parameter, including percentiles of the entire spatial frequency distribution [*Willmott et al.*, 2007; *Nickl et al.*, 2010; *Robeson et al.*, 2014], for a variable that is represented by different-sized areal units. While PDSI-derived drought estimates are the primary focus here, the October–June instrumental precipitation values also are evaluated for the same spatial averaging error, with the relative magnitude of the precipitation anomaly during 2012–2015 being compared to the reconstructed values from GA14.

To compare the spatially averaged instrumental and tree ring data, the tree-ring-derived PDSI values must be adjusted to the same scale as the instrumental PDSI during the calibration period. In this case, the calibration period is the complete period of overlap between the two data sets: 1895 to 2006. Here two procedures are compared: (1) "mean/std adjustment" of the NADA tree ring record so that it has the same mean and standard deviation (std) as the instrumental data and (2) "quantile mapping" of the empirical cumulative distribution function (cdf) of the tree ring record onto that of the instrumental data. Mean/std adjustment is the more customary procedure in dendroclimatology [*Meko*, 1997], but quantile mapping has been widely used for bias correction in a variety of contexts [e.g., *Abatzoglou and Brown*, 2012; *Maurer and Hidalgo*, 2008; *Wood et al.*, 2004]. While both mean/std adjustment and quantile mapping can be thought of as a bias correction and, therefore, produce pre-1895 PDSI values that are directly comparable to the instrumental data, the former uses just two parameters with the goal of matching the central tendency and dispersion of the two samples. Quantile mapping, on the other hand, adjusts the entire empirical cdf of one sample to that of another sample such that all of their quantiles correspond. This can be a particularly important adjustment for the estimation of extreme values. Here the NADA PDSI values underestimate PDSI of the instrumental data in the tails of their distributions—a feature that mean/std adjustment does not address (Figure S2).

After mean/std adjustment and quantile mapping the NADA PDSI values to the instrumental ones, a generalized extreme value (GEV) distribution is fit to block maxima over the 1200+ year record using maximum likelihood estimation [*Coles et al.*, 2001]. In order to use maxima, all of the PDSI values are first multiplied by −1. In extreme value analysis, the choice of block size can be important, with the compromise being between big blocks that have larger sampling errors (missed events) and small blocks that can produce biased estimates (block maxima should be independent and identically distributed). The NADA PDSI data are not highly autocorrelated nor do they have observable nonstationarities such as a long-term trend or periodicities. Even so, the sensitivity of the GEV fit is evaluated for a range of block sizes. Return periods are then calculated for the spatially weighted JJA PDSI value for 2014, 2012–2014, and 2012–2015. Data for July and August of 2015 were not yet available when these results were produced, so the spatially averaged June 2015 PDSI is used as a reliable estimate of the JJA PDSI value (Figure S3).

3. Results

Weighted spatial means of JJA PDSI for the instrumental data from central and southern California differ from the unweighted (arithmetic) mean of the four divisions (Figures 1a and 1b). Differences between the spatially weighted and unweighted mean range from −1.02 to 1.22, with a mean absolute error of 0.38 (all in PDSI units). The JJA PDSI for 2014 is −6.31, whereas the unweighted mean PDSI is −6.94, with much of the error being caused by the equal weighting of the largest division (which had a relatively less severe PDSI during 2014). As in GA14, the spatially averaged 2014 PDSI for central and southern California is the most severe in the instrumental record. Similarly, the 3 year cumulative PDSI for spatially weighted and unweighted means also differ, with errors ranging from −2.60 to 2.51 PDSI units and a mean absolute error of 0.75 PDSI units (Figures 1c and 1d). The 2012–2014 cumulative PDSI is −13.58, whereas the unweighted value is −14.55 PDSI units (this latter value is reported in GA14, confirming their use of an unweighted spatial average).

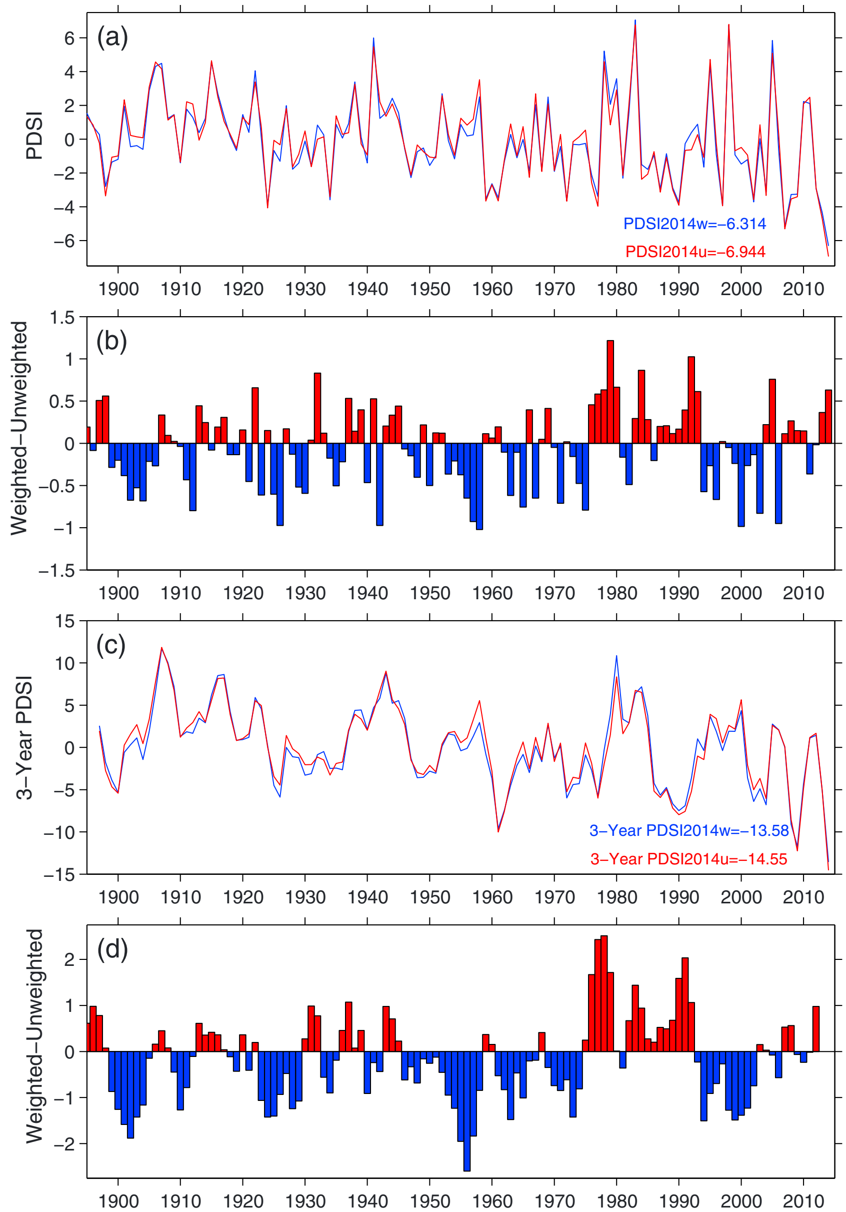

Figure 1. Time series of June/July/August average PDSI derived from California divisions 4 to 7 for 1895 to 2014: (a) using an average weighted by the area of each division (blue line) and an unweighted average (red line), (b) the difference of the 1 year weighted and unweighted averages, (c) weighted and unweighted 3 year cumulative June/July/August average PDSI, and (d) the difference of the 3 year weighted and unweighted averages.

The 2012–2014 event is the most extreme 3 year drought in the instrumental record, but the 2007–2009 drought also is severe, and its cumulative PDSI (−11.71) is closer in magnitude to the 2012–2014 drought than previously estimated (the unweighted 2007–2009 PDSI is −12.24).

Using mean/std adjustment of the spatially weighted instrumental PDSI values to scale the NADA (tree ring) record produces a time series that is similar to that assessed by GA14, but with different estimates of extreme values (Figure 2). These differences are due to a combination of the spatial averaging procedure and the more complete spatial match of NADA grid points to the whole of central and southern California (the spatially matched instrumental and tree ring data are even more highly correlated here; $r = 0.87$). Using mean/std adjustment of the NADA record to the 1895–2006 divisional record, there are 11 one year PDSI values in the preinstrumental tree ring record that are more severe than the 2014 PDSI value (Figures 2a

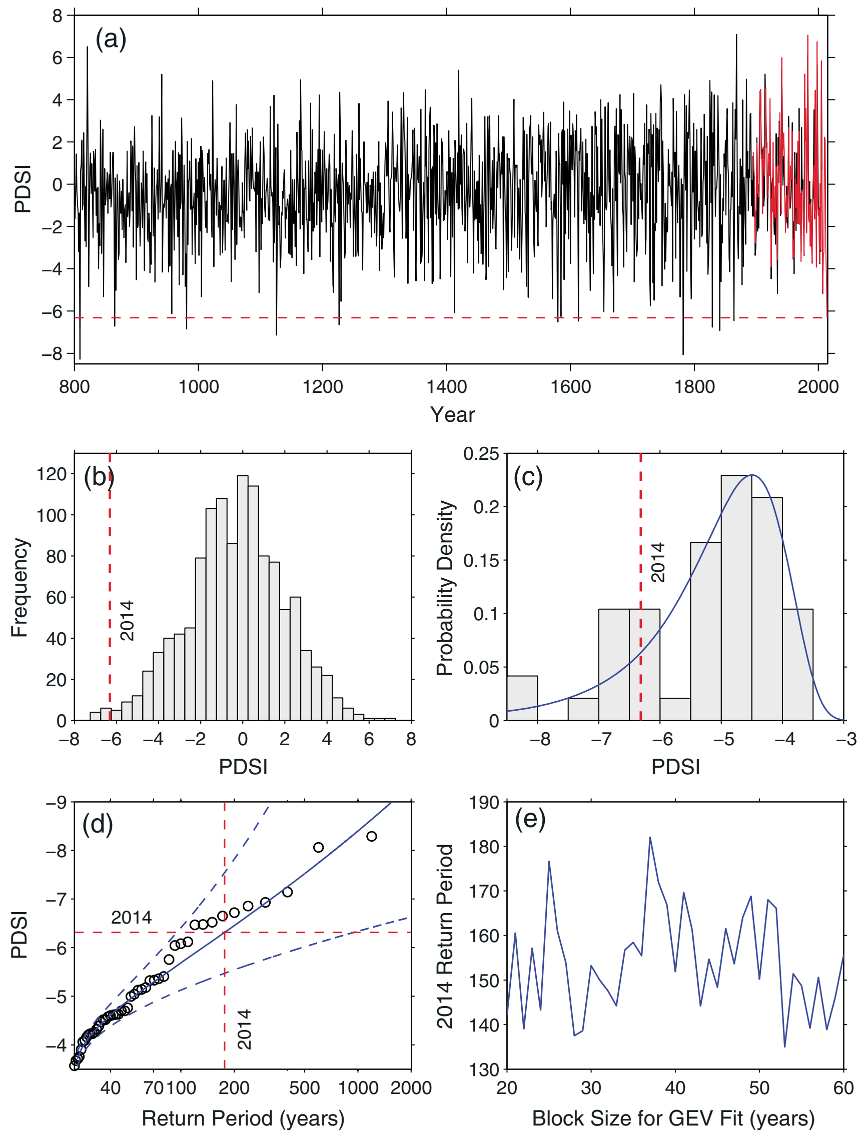

Figure 2. Time series of June/July/August average PDSI for California divisions 4 to 7: (a) comparison of the area-weighted division average (red line) and mean/std adjusted NADA grid point average (black line) for 1895–2014 ($r = 0.866$), (b) histogram of the NADA grid point averages for 800 to 2006 with the value for 2014 indicated, (c) histogram of extrema with GEV fit to 25 year block maxima (blue line), (d) return periods (blue line) and 95% confidence intervals (dashed blue lines) for 25 year block maxima, and (e) sensitivity of GEV-estimated return period to size of block maxima. Using mean/std adjustment, the 2014 event with a PDSI value of −6.31 is an extreme event, but the 1200+ year NADA tree ring record has 11 years with PDSI more extreme than the value for 2014, which has an approximate return period of 140–180 years.

and 2b; those years are 809, 865, 981, 1126, 1227, 1580, 1613, 1782, 1829, 1841, and 1864). There is just one 3 year event more severe as the 2012–2014 cumulative PDSI value: 979 to 981, but it is considerably more severe with a cumulative 3 year PDSI of −14.98. Using the standardized NADA time series, extreme value analysis of 25 year block maxima estimates the 2014 (1 year) drought to be approximately a 175 year event (Figures 2c and 2d). Sensitivity analysis of the standardized NADA data that varies the block size from 20 to 60 years shows a return period in the range of 140 to 180 years (Figure 4e). The GEV estimates are relatively insensitive to block size, and the NADA time series has low lag 1 autocorrelation, giving additional confidence to the estimated return periods.

When estimating extreme droughts, however, it is evident that mean/std adjustment does not address the bias in the lower tail of the PDSI distribution (Figure S2). As a result, the remainder of the results presented

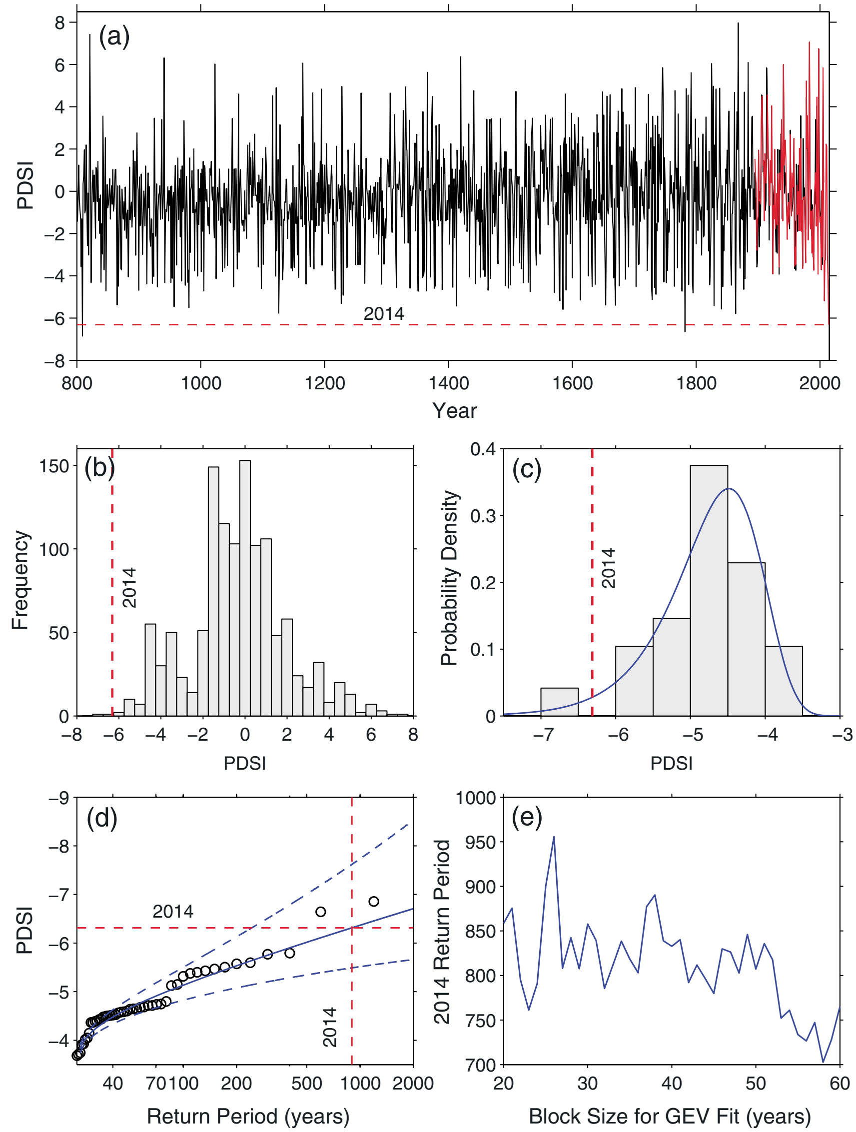

Figure 3. Time series of quantile mapped June/July/August average PDSI for California divisions 4 to 7: (a) comparison of the area-weighted division average (red line) and quantile mapped NADA grid-point average (black line) for 1895–2014 ($r = 0.874$), (b) histogram of the NADA grid point averages for 800 to 2006 with the value for 2014 indicated, (c) histogram of extrema with GEV fit to 25 year block maxima (blue line), (d) return periods (blue line) and 95% confidence intervals (dashed blue lines) for 25 year block maxima, and (e) sensitivity of GEV-estimated return period to size of block maxima. Using quantile mapping with the 1200+ year NADA tree ring record produces just 2 years with PDSI more extreme than the value for 2014. This gives an approximate return period of 800–900 years for the 1 year event.

here use quantile mapping of the spatially weighted instrumental PDSI values to scale the NADA (tree ring) record. In estimating the 1 year PDSI time series and extreme events, quantile mapping produces just 2 years with drought estimates that are more severe than the 2014 event (Figures 3a and 3b; those years are 809 and 1782). Extreme value analysis of 25 year block maxima estimates the 2014 (1 year) drought to be approximately an 800 year event (Figures 3c and 3d), while sensitivity analysis that varies the block size from 20 to 60 years shows a return period in the range of 700 to 900 years (Figure 3e). As a result, the 2014 JJA PDSI is extreme, but it is not estimated to be the most severe in the 1200+ year record.

Using quantile mapping with 3 year cumulative PDSI values produces a time series that shows 2012–2014 to be an unusually severe event (Figures 4a and 4b). There is one other 3 year period (979 to 981) with approximately the same magnitude as the 2012–2014 cumulative drought, but extreme value analysis shows that both events

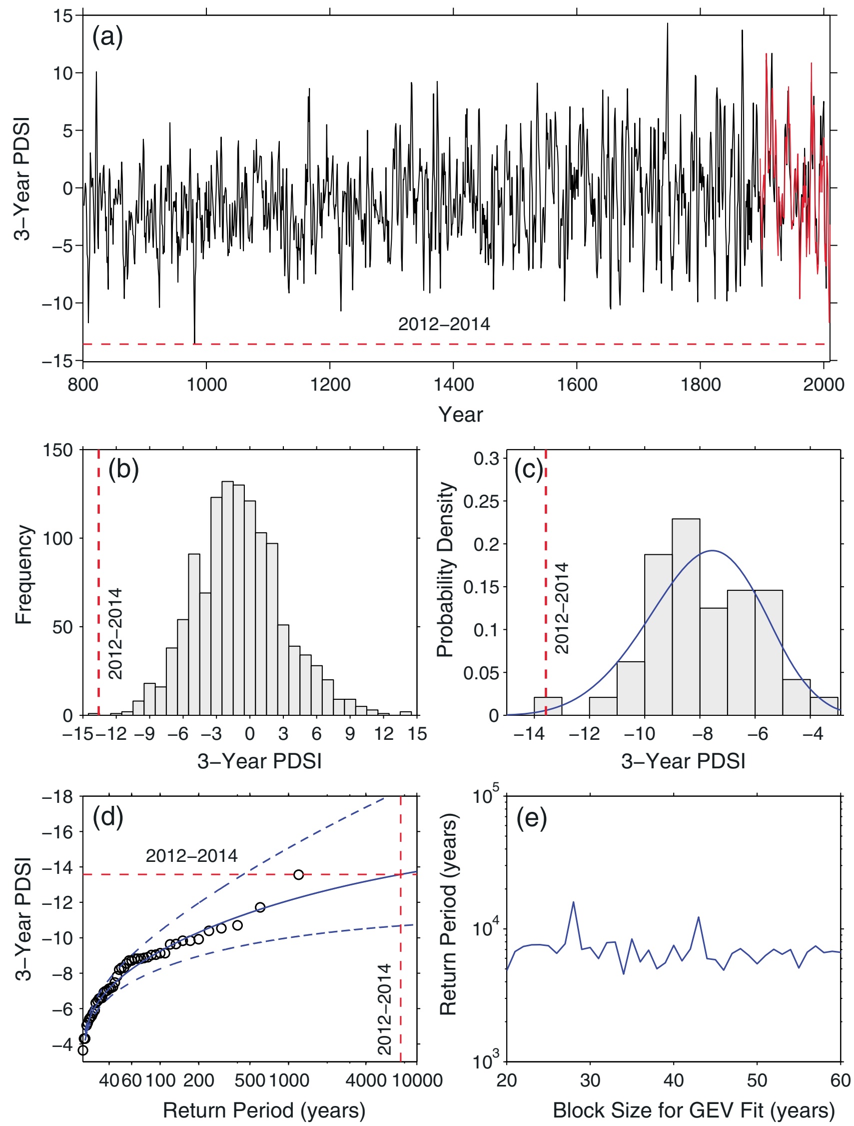

Figure 4. Analyses of cumulative 3 year JJA PDSI (using quantile mapping) for central and southern California: (a) time series of NADA-derived 3 year PDSI for 800–802 to 2004–2006 (with 3 year PDSI for divisional data shown in red); (b) histogram of NADA grid point averages for 800–802 to 2004–2006, with the value for 2012–2014 indicated; (c) histogram of extrema with GEV fit to 25 year block maxima (blue line); (d) return periods (blue line) and 95% confidence intervals (dashed blue lines) for 25 year block maxima, with the estimated return period for 2012–2014 indicated (dashed red lines); and (e) sensitivity of GEV-estimated return period to size of block maxima. One other 3 year period (979 to 981) has approximately the same magnitude as the 2012–2014 cumulative drought.

have a return period in the range of 6000 to 10,000 years (Figures 4c–4e). The 3 year cumulative PDSI time series is somewhat nonstationary with reduced variability in the early part of the record (Figure 4a), and the 3 year time series also has strong autocorrelation due to the moving summation (lag 1 autocorrelation is 0.661), so there is some additional uncertainty in the characterization of the 2012–2014 cumulative event. Overall, however, the correspondence between the 3 year divisional and NADA PDSI values during the calibration period suggests that reconstruction of 3 year PDSI is even more reliable than 1 year PDSI (Figure S4a).

Using the June 2015 PDSI to estimate the JJA 2015 PDSI allows for a close approximation of the magnitude of the 2012–2015 cumulative drought (Figure S3). In addition, 4 year droughts are very reliably estimated during the calibration period (Figure S4b). Using quantile mapping and extreme value analysis, the 2012–2015

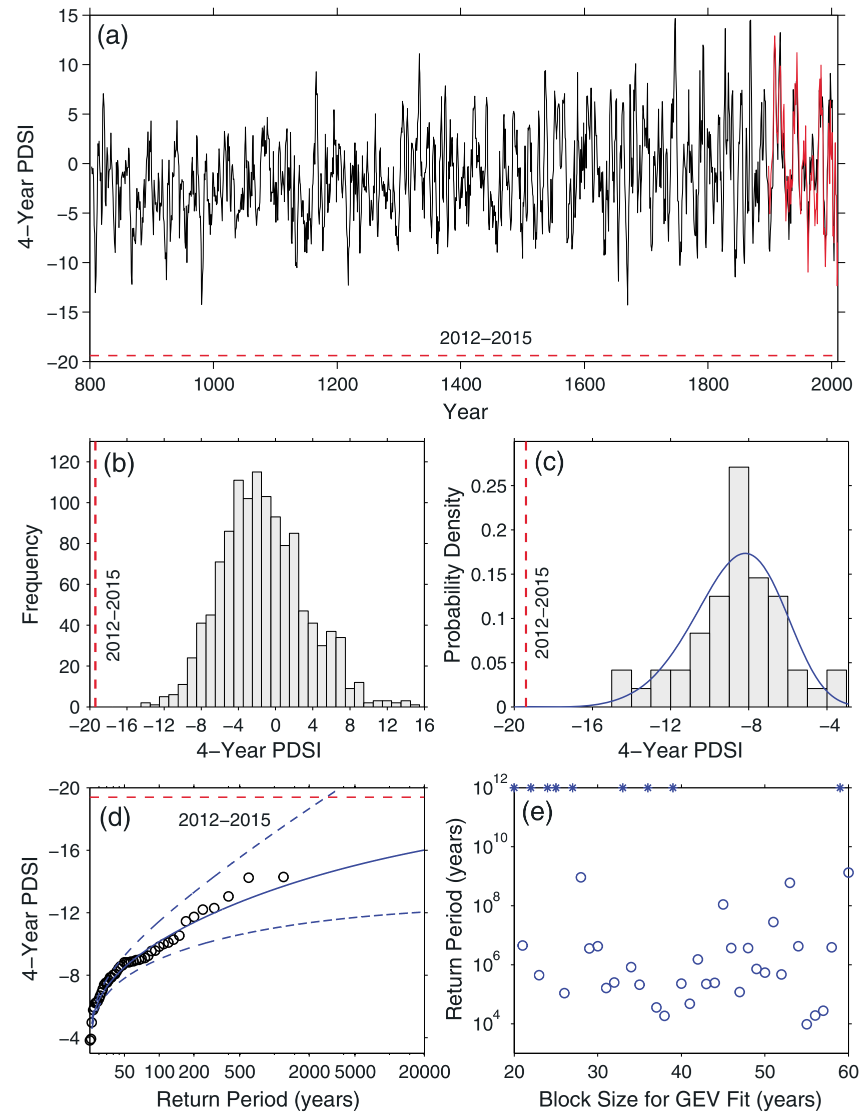

Figure 5. Analyses of cumulative 4 year JJA PDSI (using quantile mapping) for central and southern California: (a) time series of NADA-derived 4 year PDSI for 800–803 to 2003–2006; (b) histogram of NADA grid point averages for 800–803 to 2003–2006, with the estimate value for 2012–2015 indicated (the JJA value for 2015 derives from the June 2015 PDSI); (c) histogram of extrema with GEV fit to 25 year block maxima (blue line); (d) return periods (blue line) and 95% confidence intervals (dashed blue lines) for 25 year block maxima; and (e) sensitivity of GEV-estimated return period to size of block maxima (blocks that produced infinite return periods are indicated with an asterisk). All panels suggest that the 2012–2015 cumulative PDSI has no precedent in the last 1200+ years.

cumulative drought is estimated to be a completely unprecedented 4 year event (Figure 5). The next closest event was from 978 to 981 but has a 4 year cumulative PDSI that is ≈ 5 PDSI units higher (Figure 5b). The magnitude of the 4 year 2012–2015 value is so large that return period estimates represent an extraordinary extrapolation of reconstructed PDSI and, therefore, vary widely (Figure 5e). Some GEV fits asymptote to zero below the PDSI for the 2012–2015 event and, therefore, produce infinitely large return periods (Figures 5c and 5d). Over all block sizes, even the lowest return period estimates exceed 10,000+ years (Figure 5e). By making an arguably more appropriate bias adjustment to the lower tail of the NADA PDSI distribution, quantile mapping makes the 2012–2015 event more unusual. The same approach using traditional mean/std adjustment, however, also produces multimillenial return periods for the 2012–2015 drought, supporting the robustness of these results (Figure S5).

While the primary focus here is on estimating extreme values of PDSI, the instrumental October to June precipitation values in GA14 also are not weighted by the divisional areas. Errors for 1 year standardized precipitation anomalies are relatively small, particularly for the 2014 value, but they are larger for accumulated values such as 3 year sums (Figure S6). As in GA14, the spatially weighted 2014 standardized precipitation anomaly is not unusually low (−1.42). Here, however, the 3 year 2012–2014 standardized precipitation anomaly when using quantile mapping is barely lower than any other 3 year value in the 800+ year record (Figure S7). In addition, both bias removal procedures produce a 4 year October–June 2012–2015 precipitation anomaly that is even more unusual than the 3 year one (Figure S8). Obviously, GA14 did not have access to 2015 data, so this result extends their analysis. As a result, precipitation during 2012–2015 also is unprecedented in the paleorecord, but the 4 year PDSI value is more extreme than the 4 year precipitation anomaly.

4. Summary and Discussion

The estimation of the magnitude of extreme droughts over central and southern California is influenced by the way that spatial averages are constructed (Figure 1) and the choice of bias adjustment procedure (compare Figures 2 and 3). When analyzed over the entirety of central and southern California, the spatially averaged JJA PDSI value for 2014 and for 2012–2014 are the most severe in the instrumental record (Figure 1), but the most commonly used bias adjustment procedure produces a times series that ranks 2014 outside the top 10 of extreme droughts in the 1200+ tree ring record (Figure 2) A more sophisticated correction of the tree ring data—quantile mapping—identifies just two historical events that are more severe than the 1 year 2014 drought (Figure 3) and estimates the cumulative 2012–2014 drought as the most severe 3 year drought in the last 1200+ years (Figure 4). When quantile mapping is applied to cumulative 4 year droughts, however, the 2012–2015 PDSI in central and southern California is estimated to be unprecedented in the 1200+ year record, with its return period being almost incalculably large (Figure 5).

Regarding the statistical confidence in estimates of extreme droughts, there is both sampling- and calibration-induced uncertainty. While dimensioned error measures such as RMSE (root-mean-squared error) are useful measures of overall calibration uncertainty, they are not as useful in the tails of distributions. In addition, RMSE is independent of sample size, indicating that an approach that evaluates sampling error in the lower tail of the PDSI distribution also is needed. Here the magnitude of sampling-induced uncertainty in the lower PDSI tail is illustrated in the confidence intervals associated with the extreme value distributions (Figures 2–5). Even at a 95% confidence level, the lower bound of the 2012–2014 cumulative drought is estimated as a 500+ year event (Figure 4d), and the 2012–2015 cumulative drought has a lower bound of 2000+ years (Figure 5d). Even though the reduced network of tree ring chronologies in the early centuries of the 1200+ year record make those PDSI values more uncertain [*Cook et al.*, 2008], the 4 year drought from 2012 to 2015 is so large in magnitude that no other drought event in the tree ring record comes close to its severity (Figure 5).

Moving forward, ongoing changes in atmospheric circulation and associated precipitation and temperature variability in the western U.S. [*Seager et al.*, 2007; *Swain et al.*, 2014] raise questions about the stationarity of extreme drought estimates. Adaptive approaches [*Huerta and Sansó*, 2007; *Katz*, 2010; *Towler et al.*, 2010] should be useful in estimating time-varying parameters, but disentangling past relationships between precipitation, temperature, and drought variability in California also will require incorporating additional tree ring chronologies and spatial analyses that use higher resolution instrumental data rather than the coarser divisional data. Representations of PDSI that do not rely primarily on temperature-derived potential evapotranspiration also will be valuable in evaluating the causes of drought variability [*Sheffield et al.*, 2012; *Yuan and Quiring*, 2014]. However, given the cumulative magnitude of recent drought conditions, nearly any analysis of the 2012–2015 drought will demonstrate its unprecedented severity. Continued monitoring and analysis will evaluate whether such extreme droughts will occur more frequently in a changing California climate.

Acknowledgments
The data used here (instrumental, NADA, and GA14 reconstructions) are available from NOAA's National Centers for Environmental Information. I appreciate the contributions of the many cooperative observers and tree ring researchers who worked to produce these data. Chunfeng Huang and Cort Willmott, as well as the anonymous reviewers, provided valuable comments on early drafts. I also appreciate conversations with John Abatzoglou regarding quantile mapping and with Dan Griffin and Kevin Anchukaitis regarding their work that inspired this research.

The Editor thanks three anonymous reviewers for their assistance in evaluating this paper.

References

Abatzoglou, J. T., and T. J. Brown (2012), A comparison of statistical downscaling methods suited for wildfire applications, *Intl. J. Climatol.*, *32*(5), 772–780.

Coles, S., J. Bawa, L. Trenner, and P. Dorazio (2001), *An Introduction to Statistical Modeling of Extreme Values*, vol. 208, Springer, London.

Cook, E. R., C. A. Woodhouse, C. M. Eakin, D. M. Meko, and D. Stahle (2004), Long-term aridity changes in the western United States, *Science*, *306*(5698), 1015–1018.

Cook, E. R., U. Lall, C. Woodhouse, and D. M. Meko (2008), North American Summer PDSI Reconstructions, Version 2a. IGBP PAGES/World Data Center for Paleoclimatology Data Contribution Ser. 2008–046, NOAA/NGDC Paleoclimatology Program, Boulder, Colo.

Diffenbaugh, N. S., D. L. Swain, and D. Touma (2015), Anthropogenic warming has increased drought risk in California, *Proc. Natl. Acad. Sci.*, *112*(13), 3931–3936.

Funk, C., A. Hoell, and D. Stone (2014), Examining the contribution of the observed global warming trend to the California droughts of 2012/13 and 2013/14, *Bull. Am. Meteorol. Soc.*, *95*(9), S11–S15.

Griffin, D., and K. J. Anchukaitis (2014), How unusual is the 2012–2014 California drought?, *Geophys. Res. Lett.*, *41*, 9017–9023, doi:10.1002/2014GL062433.

Guttman, N. (1998), Comparing the Palmer Drought Index and the Standardized Precipitation Index, *J. Am. Water Resour. Assoc.*, *34*, 113–121.

Heim, R. R., Jr. (2005), Computing the monthly Palmer Drought Index on a weekly basis: A case study comparing data estimation techniques, *Geophys. Res. Lett.*, *32*, L06401, doi:10.1029/2004GL022118.

Huerta, G., and B. Sansó (2007), Time-varying models for extreme values, *Environ. Ecol. Stat.*, *14*(3), 285–299.

Katz, R. W. (2010), Statistics of extremes in climate change, *Clim. Change*, *100*(1), 71–76.

Maurer, E. P., and H. G. Hidalgo (2008), Utility of daily vs. monthly large-scale climate data: An intercomparison of two statistical downscaling methods, *Hydrol. Earth Syst. Sci.*, *12*(2), 551–563.

Meko, D. (1997), Dendroclimatic reconstruction with time varying predictor subsets of tree indices, *J. Clim.*, *10*(4), 687–696.

Nickl, E., C. J. Willmott, K. Matsuura, and S. M. Robeson (2010), Changes in annual land-surface precipitation over the 20th and early 21st century, *Ann. Assoc. Am. Geogr.*, *100*, 1–11.

Robeson, S. M., C. J. Willmott, and P. D. Jones (2014), Trends in hemispheric warm and cold anomalies, *Geophys. Res. Lett.*, *41*, 9065–9071, doi:10.1002/201GL062323.

Seager, R., et al. (2007), Model projections of an imminent transition to a more arid climate in southwestern North America, *Science*, *316*(5828), 1181–1184.

Sheffield, J., E. F. Wood, and M. L. Roderick (2012), Little change in global drought over the past 60 years, *Nature*, *491*, 435–438, doi:10.1038/nature11575.

Swain, D. L., M. Tsiang, M. Haugen, D. Singh, A. Charland, B. Rajaratnam, and N. S. Diffenbaugh (2014), The extraordinary California drought of 2013/2014: Character, context, and the role of climate change, *Bull. Am. Meteorol. Soc.*, *95*(9), S3–S7.

Towler, E., B. Rajagopalan, E. Gilleland, R. S. Summers, D. Yates, and R. W. Katz (2010), Modeling hydrologic and water quality extremes in a changing climate: A statistical approach based on extreme value theory, *Water Resour. Res.*, *46*, W11504, doi:10.1029/2009WR008876.

Vose, R. S., S. Applequist, M. Squires, I. Durre, M. J. Menne, C. N. Williams, C. Fenimore, K. Gleason, and D. Arndt (2014), Improved historical temperature and precipitation time series for U.S. climate divisions, *J. Appl. Meteorol. Climatol.*, *53*(5), 1232–1251, doi:10.1175/jamc-d-13-0248.1.

Willmott, C. J., S. M. Robeson, and K. Matsuura (2007), Geographic box plots, *Phys. Geogr.*, *28*, 331–344.

Wood, A. W., L. R. Leung, V. Sridhar, and D. P. Lettenmaier (2004), Hydrologic implications of dynamical and statistical approaches to downscaling climate model outputs, *Clim. Change*, *62*, 189–216.

Yuan, S., and S. M. Quiring (2014), Drought in the U.S. Great Plains (1980–2012): A sensitivity study using different methods for estimating potential evapotranspiration in the Palmer Drought Severity Index, *J. Geophys. Res. Atmos.*, *119*, 10,996–11,010, doi:10.1002/2014JD021970.